Sequential Interpenetrating Polymer Networks of Novolac Resin and Poly(*n*-butyl methacrylate)

Sudipta Goswami and Debabrata Chakrabarty

Department of Polymer Science and Technology, University College of Science and Technology, Kolkata 700 009, India

Received 2 December 2005; accepted 19 January 2006
DOI 10.1002/app.24182
Published online in Wiley InterScience (www.interscience.wiley.com).

ABSTRACT: Novolac resin/poly(*n*-butyl methacrylate), P(*n*-BMA), sequential interpenetrating polymer networks (both semi and full types) were prepared and characterization of the various compositions (up to 40% by weight of PF incorporation) was performed in terms of mechanicals, namely, ultimate tensile strength (UTS), percentage elongation at break (% E.B.), modulus, and toughness. Thermal properties were studied by differential scanning calorimetry and thermogravimetric analysis (TGA). Crosslink densities of the IPNs were calculated using Flory-Rehner equation. The morphological features were studied through scanning electron microscope. There was a gradual decrease of modulus and UTS with consequent increases in % E. B. and toughness with increasing proportions of P(*n*-BMA). An inward shifting and lowering of the glass transition temperatures of the IPNs (compared with that of pure phenolic resin) with increasing proportions of P(*n*-BMA) were observed. The TGA thermograms exhibit two-step degradation patterns. A typical cocontinuous bi-phasic morphology is evident in the micrographs. © 2006 Wiley Periodicals, Inc. J Appl Polym Sci 102: 4030–4039, 2006

Key words: brittle; interpenetrating networks; differential scanning calorimetry (DSC); FTIR; crosslinking

INTRODUCTION

Interpenetrating polymer networks can be defined as a unique alloy of two polymers (either one or both of them may be crosslinked), catenated physically by two independent and noninterfering polymerization reactions.[1–3] These are considered as self-organizing systems because their formation occurs under nonequilibrium conditions.[4,5] The simultaneous processes of reaction and phase separation are typical for IPNs, with the phase separation resulting from the incompatibility of the growing chains formed *in situ*. The effect of network interlock during interpenetrating polymer network formation not only provides a sterically hindered environment for the curing reactions but also restrains the chain mobilities of the respective components, leading to lower rate constants of polymerization and higher activation energies during IPN formation.[6,7] However, the increased network interlocking is expected to improve compatibility between the components involved in IPN formation. The ultimate properties of IPNs are dependent on the two-phase morphology that develops during polymerization/crosslinking processes of either phase. The morphology of IPNs varies with degree of crosslinking and the sequence of formation of the two networks.[8–10] For the sequential IPNs, as is observed in the present case, the continuous network dictates the properties.[11] The limited phase separation caused by the unique microstructure of IPNs broadens the glass transition regions of the component networks and can merge them into a single transition covering a wide temperature range.[12,13] It is this broad transition range that makes IPNs likely candidates for high-damping applications.[14]

The present study aims at improvement of toughness of phenol-formaldehyde resin by blending it with poly(*n*-butyl methacrylate) (P(*n*-BMA)) by the IPN formation. The rubber-toughening influence of elastomeric P(*n*-BMA) on the continuous brittle matrix of phenolic resin is investigated as a function of P(*n*-BMA) content.

EXPERIMENTAL

Materials

Novolac, the precursor of the crosslinked phenolic resin mixed with 10% (of the novolac resin weight) of hexamethylene tetramine (HEXA), was procured from Hindustan Adhesives (Kolkata, India) and used without further modification. The monomer (*n*-butyl methacrylate, BMA), from Berger Paints, India Ltd., was purified by washing first with 2% aqueous sodium hydroxide (NaOH) solution and then by thorough and repeated washings with distilled water (to

Correspondence to: D. Chakrabarty (d chakraborty@vsnl.net).

make alkali free, as tested by litmus paper) and dried over fused calcium chloride ($CaCl_2$), after which it was finally vacuum distilled. Benzoyl peroxide (Bz_2O_2) from B.D.H. India was purified by repeated crystallization from chloroform. 2-Ethyl-2-(hydroxymethyl)-1,3-propanediol trimethacrylate (Aldrich Chemical, Milwaukee, WI), without any modification, was used as comonomer and crosslinker for P(*n*-BMA).

IPN synthesis

A weighed amount of purified acrylic monomer was placed in a test tube and thoroughly mixed with 2% by weight (based on the monomer) of recrystallized Bz_2O_2. The novolac resin (premixed with HEXA in the proportion required for its complete curing) was weighed in a glass jar to maintain a suitable ratio with the acrylic monomer as weighed earlier. The contents of the test tube were then poured into the jar and mixed thoroughly and uniformly until the mixture turned almost to a paste. However, with an increase in acrylic monomer content, the consistency of the paste became diluted. The resulting mass was then allowed to mature for about 2 h. The paste was then transferred into a positive type compression sheet mold, which was preheated to 80°C. The mold was then closed and placed on the lower platen of the hydraulic press. The press was then closed with a mild pressure to keep the mold airtight and to ensure that no air was entrapped into the sheet. This condition was maintained for 30 min to allow the acrylic polymerization to initiate and propagate to a certain extent. Once the stipulated time period for the acrylic polymerization was over, the pressure of the mold was increased to 5 tons/cm^2 and the mold was kept under such conditions for 30 min, which ensured complete crosslinking of the phenolic resin and complete polymerization of acrylic as well. The mold was then removed from the press in hot condition and opened cautiously so that there was no distortion and warpage of the sheet. Samples for testing were cut from the sheet after maturing for 7 days. In the case of full IPNs, the comonomer crosslinker was added (2% w/w with respect to the acrylic monomer taken) into the BMA monomer before the addition of novolac resin. All other steps remained unaltered.

Characterization

Mechanical properties

An Instron Universal Testing Machine (Model 4204) was used for measuring the tensile properties, such as ultimate tensile strength (UTS), percentage elongation at break (% E.B.), modulus, and toughness. The ASTM D 638 method was followed. A crosshead speed of 5 mm/min was maintained. All testings were conducted at room temperature. The toughness of the IPN samples was determined from the area under the load versus elongation plot. The samples were visually inspected before measurements and were found to be free from pores or nicks. The data reported are averages of at least six measurements.

Hardness of different samples were measured by means of shore D Durometer following ASTM D 2240–64T method.

Physical properties

Specific gravity values of the different IPNs were measured at room temperature using hydrostatic technique following ASTM D 792.

Crosslink densities of the IPNs in present case were determined in terms of the molecular weight between two successive crosslinks, M_c, using the well-known Flory-Rehner eq. (1), as follows,

$$M_c = \frac{V_s d_r (V_p^{1/3} - V_p/2)}{V_p + \chi V_p^2 + \ln(1 - V_p)} \quad (1)$$

where V_p is the volume fraction of polymer in the swollen mass, V_s is the molar volume of the solvent, d_r is the density of the polymer, and χ is the polymer solvent interaction parameter.

For each sample, equilibrium swelling was carried out using acetone as the solvent at a temperature of 27°C.

Equilibrium swelling was done at 27°C using nine different liquids ranging in their solubility parameter from 14.1 to 25.2 Mpa$^{1/2}$.

The swelling coefficient Q was calculated using eq. (2).

$$Q = (m - m_o)/m_o \times d_r/d_s \quad (2)$$

where m is the weight of the swollen sample, m_o is the original weight of the sample, and d_s is the density of the solvent.

The parameter V_p was found out by using eq. (3).

$$V_p = 1/1 + Q \quad (3)$$

In the subsequent plots of Q versus δ values for different solvents, the solubility parameter corresponding to the maximum value of Q was noted and this value was taken as the solubility parameter of the concerned blend system. The polymer–solvent interaction parameter was then calculated from Bristow and Watson eq. (6) as given below:

$$\chi = \beta + (V_s/RT) \times (\delta_s - \delta_p)^2 \quad (4)$$

where β is the lattice constant, 0.34, R is the universal gas constant, T is the absolute temperature, and δ_s and δ_p are solubility parameter of the solvent and the IPN sample respectively.

Gelling behavior of pure novolac resin and its various blends with the acrylate were determined as per ASTM D 2471.

Thermal properties

Thermogravimetric analysis (TGA) thermograms were obtained on a Perkin–Elmer Delta Series TGA 7 thermogravimetric analyzer (Perkin–Elmer Cetus Instruments, Norwalk, CT), under nitrogen atmosphere at a heating rate of 20°C/min. The samples ranging between 6 and 10 mg in weight were used for the TGA.

A Du Pont 2100 instrument (Du pont, Boston, MA) was used for the differential scanning calorimetry (DSC) studies. DSC scans were taken at the heating rate of 10°C/min under a continuous flow of nitrogen.

Morphology

Phase morphology was examined by a scanning electron microscope (SEM; JEOL, Japan).

RESULTS AND DISCUSSION

Mechanical properties

The various mechanical properties of the semi and full IPNs of the novolac- P(*n*-BMA) system are compared as a function of blend compositions in Figures 1–5. An interesting behavior in the variations of various mechanicals of these IPNs is that at higher concentrations of P(*n*-BMA) the differences in moduli (Fig. 1) and UTS (Fig. 2) for the semi and full IPNs of corresponding compositions appear to be gradually wider. This may be attributed to the inclusion of bulky P(*n*-BMA) molecules in between the novolac chains, lowering the crosslink density of phenolic resin to a greater extent. In the case of full IPNs, comparatively compact domains of crosslinked P(*n*-BMA) than the uncrosslinked one in case of semi IPNs might have reduced the possibility of shielding of the methylol groups on the novolac chains thereby increasing the probability of crosslinking within itself to some extent. Again, the degree of interpenetration is least favored, in this situation, because of the arrested mobility of the previously formed and *in situ* crosslinked P(*n*-BMA). Thus, the combined effects of compact, crosslinked dispersed domains of P(*n*-BMA) and the relatively smaller extent of interpenetration in case of the full IPNs appears to be more predominant over the small threading influences of the phase separated linear P(*n*-BMA) domains present in semi IPNs.

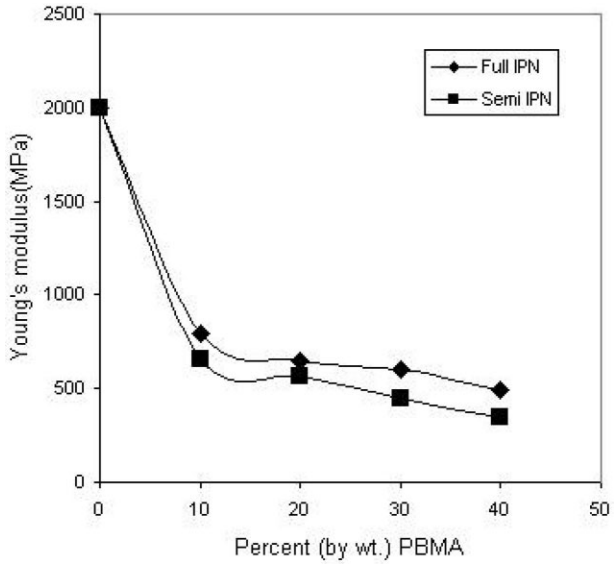

Figure 1 Variation of Young's modulus of novolac-PBMA semi and full IPNs with variation of novolac-PBMA blend ratios (w/w).

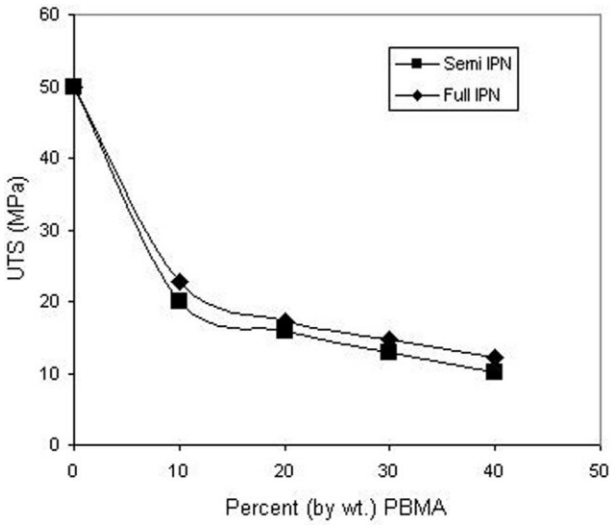

Figure 2 Variation of UTS of novolac-PBMA semi and full IPNs with variation of novolac-PBMA blend ratios (w/w).

There is a progressive increase in both % E.B. and toughness with increase in P(*n*-BMA) content. Also, it can be seen from the Figures 3 and 4, that both % E.B. and toughness of full IPNs respectively, are lower than those of the corresponding semi IPNs. Furthermore, the rate of increase of these properties for the semi IPNs is found to be much more pronounced when compared with that of the full ones. The mobility of the P(*n*-BMA) domains and consequently its ability to undergo threading with the phenolic network vis-a-vis the smaller chain extensibility of the crosslinked P(*n*-BMA) networks as encountered with full IPNs do not allow them to undergo extension. On the other hand, it has been possible with semi IPNs by virtue of chain slippage of un-

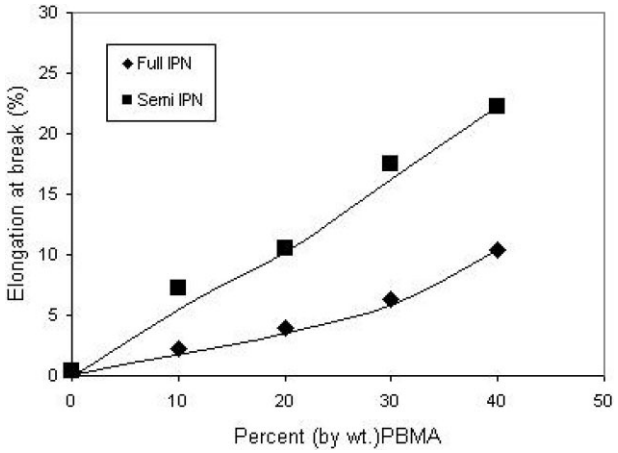

Figure 3 Variation of % E.B. of novolac-PBMA semi and full IPNs with variation of novolac-PBMA blend ratios (w/w).

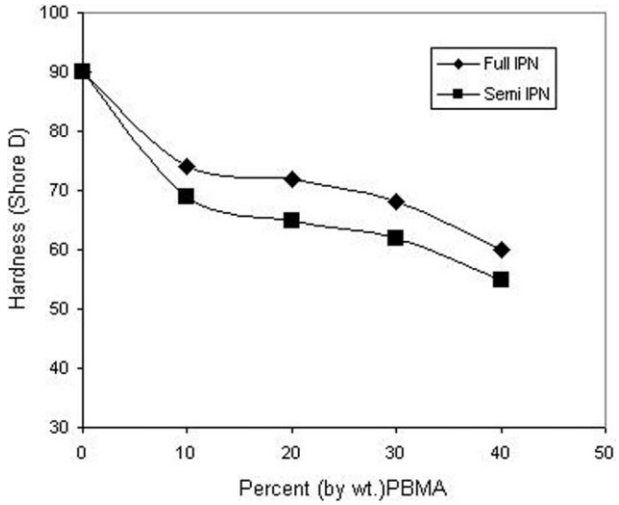

Figure 5 Variation of hardness of novolac-PBMA semi and full IPNs with variation of novolac-PBMA blend ratios (w/w).

crosslinked P(*n*-BMA) molecules through the perturbed crosslinked network of phenolics, which might possibly be accounted for the earlier observation.

Moreover, it may be expected that the linear and somewhat bulky P(*n*-BMA) domains of the semi IPNs are capable of undergoing deformation larger than the full IPNs upon application of load and allow the dissipation of energy through the interphase between the dispersed domains and the matrix, thereby increasing toughness significantly. On the other hand, crosslinked and therefore compact domains of P(*n*-BMA) in full IPNs are not able to stretch in this way and increase in toughness with increase in P(*n*-BMA) content in these IPNs is insignificant.

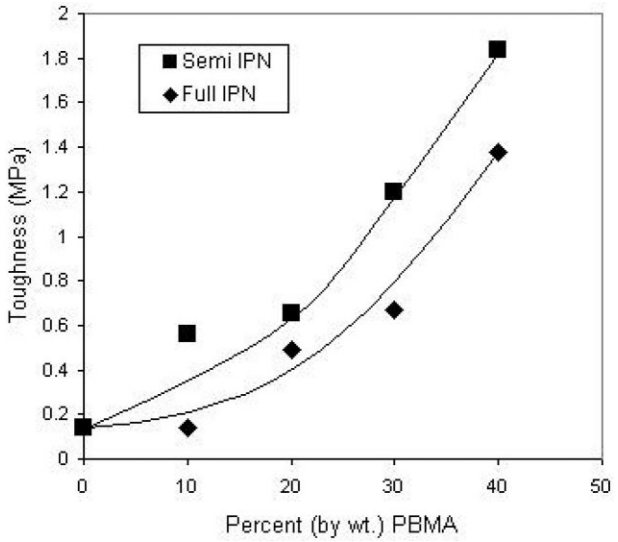

Figure 4 Variation of toughness of novolac-PBMA semi and full IPNs with variation of novolac-PBMA blend ratios (w/w).

Within the concentration range studied, the hardness decreases for both semi and full IPNs with increases in P(*n*-BMA) content (Fig. 5). The semi IPNs, however, possess lower hardness values than those for full IPNs. However, an interesting feature is observed in the hardness curves for novolac-P(*n*-BMA) IPNs. The decrease in hardness with increase in P(*n*-BMA) concentration is gradual up to 30% of P(*n*-BMA) incorporation and beyond that there is an abrupt reduction in hardness values. This may possibly be attributed to the fact that P(*n*-BMA) after a certain threshold concentration might undergo gross phase separation.

Physical properties

Specific gravity

Specific gravity versus composition curves for novolac resin-P(*n*-BMA) semi and full IPNs (Fig. 6) have shown lowering in the values of specific gravities when compared with that of theoretically expected values as drawn based on additivity rule. Entrapment of large molecules of randomly coiled P(*n*-BMA), which is assumed to possess larger free volume, in between the phenolic chains might be causing the reduction in density. This reason may possibly be coupled with the fact that the P(*n*-BMA) chains might not be allowing the novolac crosslinking to occur freely. In case of full IPNs, however, these P(*n*-BMA) chains being themselves crosslinked and compact, the statistical probability of phenolic crosslinking increases and thereby increase in the mass per unit volume for them is quite normal.

Crosslink density

The variation of M_c (i.e., average molecular weight of the polymer segments in between two successive

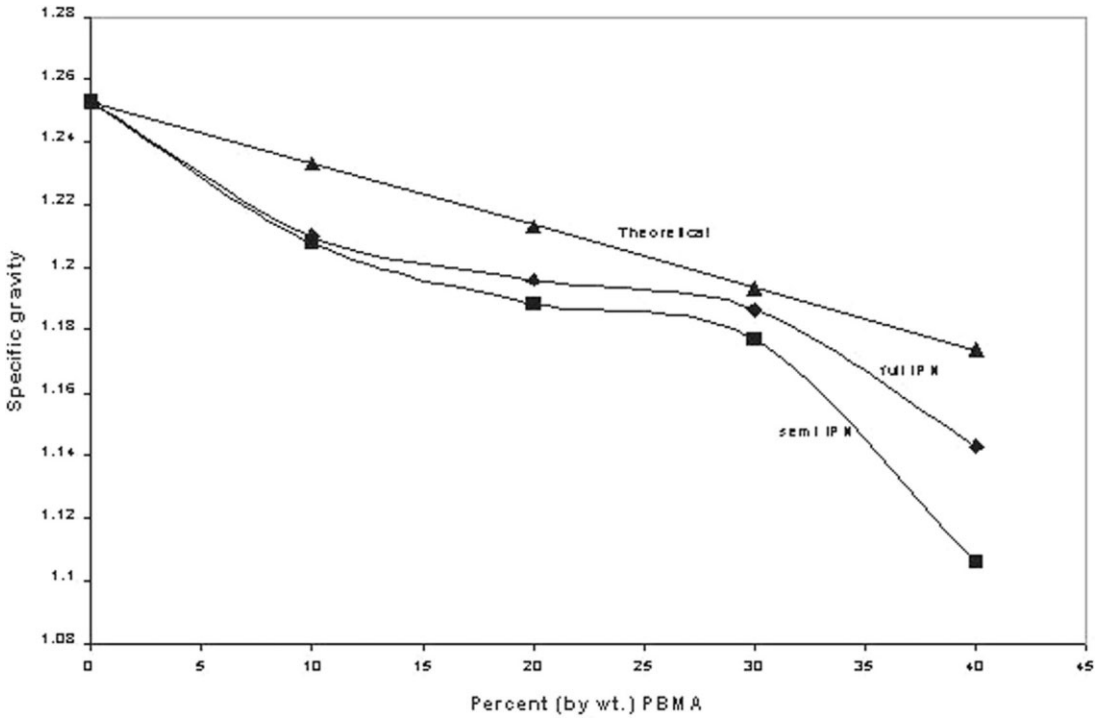

Figure 6 Variation of specific gravity of novolac-PBMA semi and full IPNs with variation of novolac-PBMA blend ratios (w/w).

crosslinks) values of both the full and semi IPNs with the P(*n*-BMA) concentration in various IPN systems is shown in Figure 7. With increase in P(*n*-BMA) content in the IPNs, there is a gradual increase in M_c i.e., decrease in the crosslink density. This may be attributed to the increase in the interchain distances of the novolac molecules due to inclusion of more and more P(*n*-BMA) formed *in situ*, which may not allow the reactive sites of

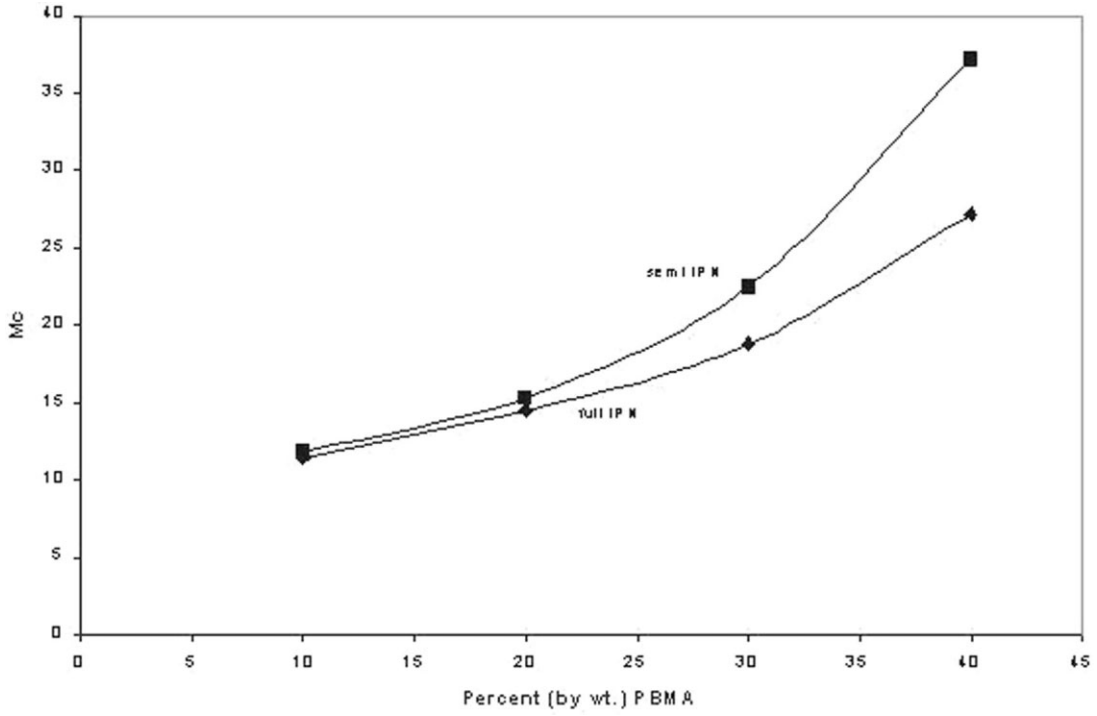

Figure 7 Variation of M_c of novolac-PBMA semi and full IPNs with variation of novolac-PBMA blend ratios (w/w).

TABLE I
DSC Results of Novolac Resin-P(*n*-BMA) Semi and Full IPNs

Sample	Composition Novolac: P(*n*-BMA) (w/w)	T_g (K)
Pure Novolac	100:0	488
Novolac-P(*n*-BMA) semi IPNs	90:10	447
	80:20	442
	70:30	439
	60:40	419
Novolac-P(*n*-BMA) full IPNs	90:10	452
	80:20	445
	70:30	439
	60:40	436
Pure P(*n*-BMA)	0:100	293

the novolac chains to approach each other to form the necessary bridge, through crosslinking reaction. As a result, the number of crosslinks per chain decreases, which in turn increases the average molecular weight in between two successive crosslinks. However, the increase in the M_c at higher concentration (beyond 30%) of P(*n*-BMA) is remarkable when compared with that at lower concentrations.

Gelling behavior

Figure 8 depicts the variation of gel time for the novolac resin-P(*n*-BMA) semi and full IPNs with composition. Increase in P(*n*-BMA) concentration in the IPNs has been accompanied by delay in gelation. Also, the full IPNs when compared with that of the semi IPNs experience longer gelation time.

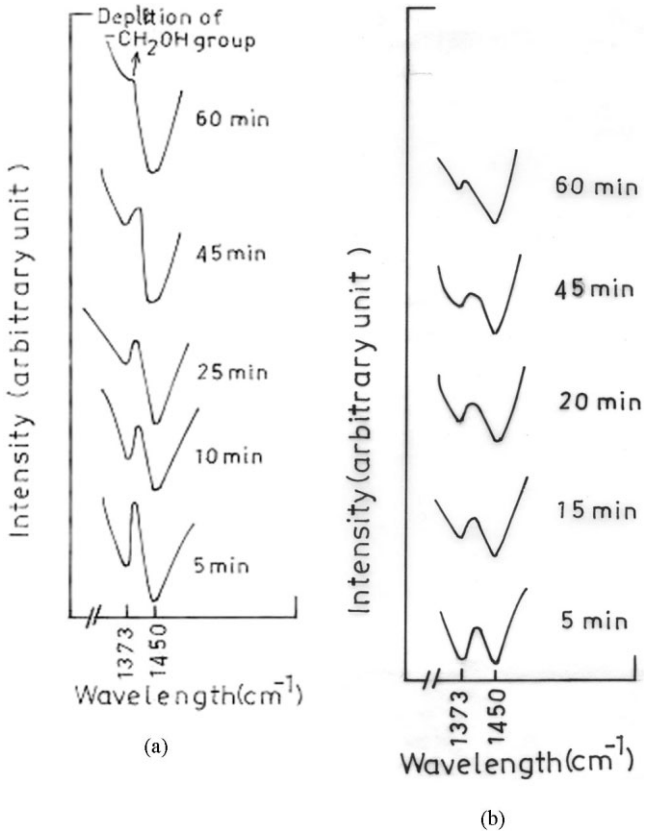

Figure 9 (a) FTIR studies on pure PF, schematic representation of depletion of —CH_2OH group. (b) FTIR studies on novolac-PBMA semi IPN containing 30% of PBMA, schematic representation of depletion of —CH_2OH group.

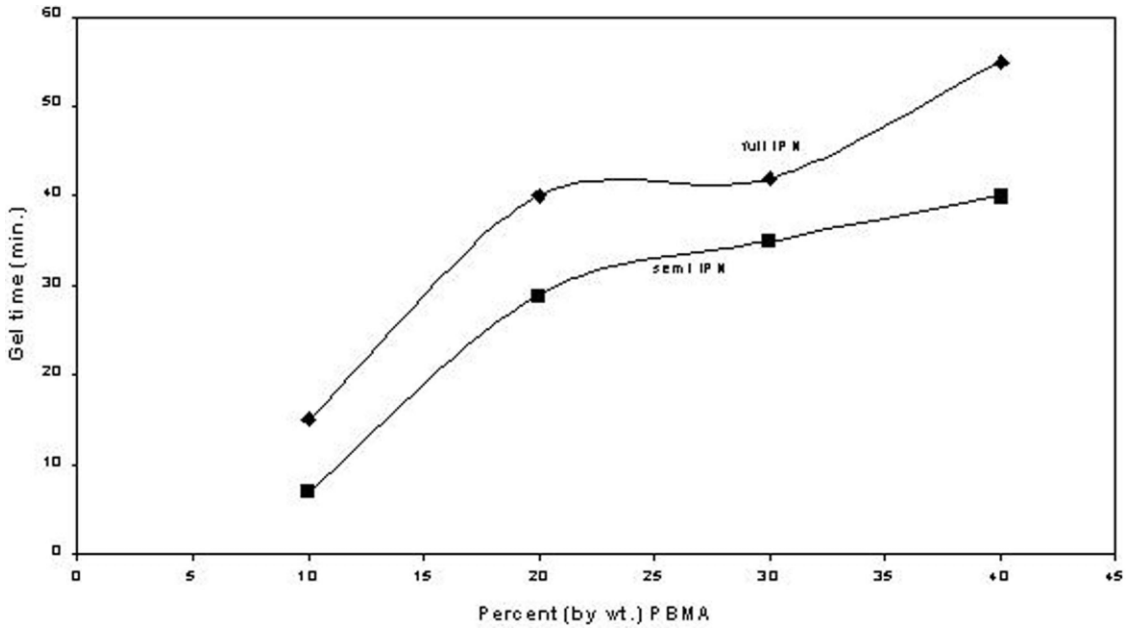

Figure 8 Variation of gel time of novolac-PBMA semi and full IPNs with variation of novolac-PBMA blend ratios (w/w).

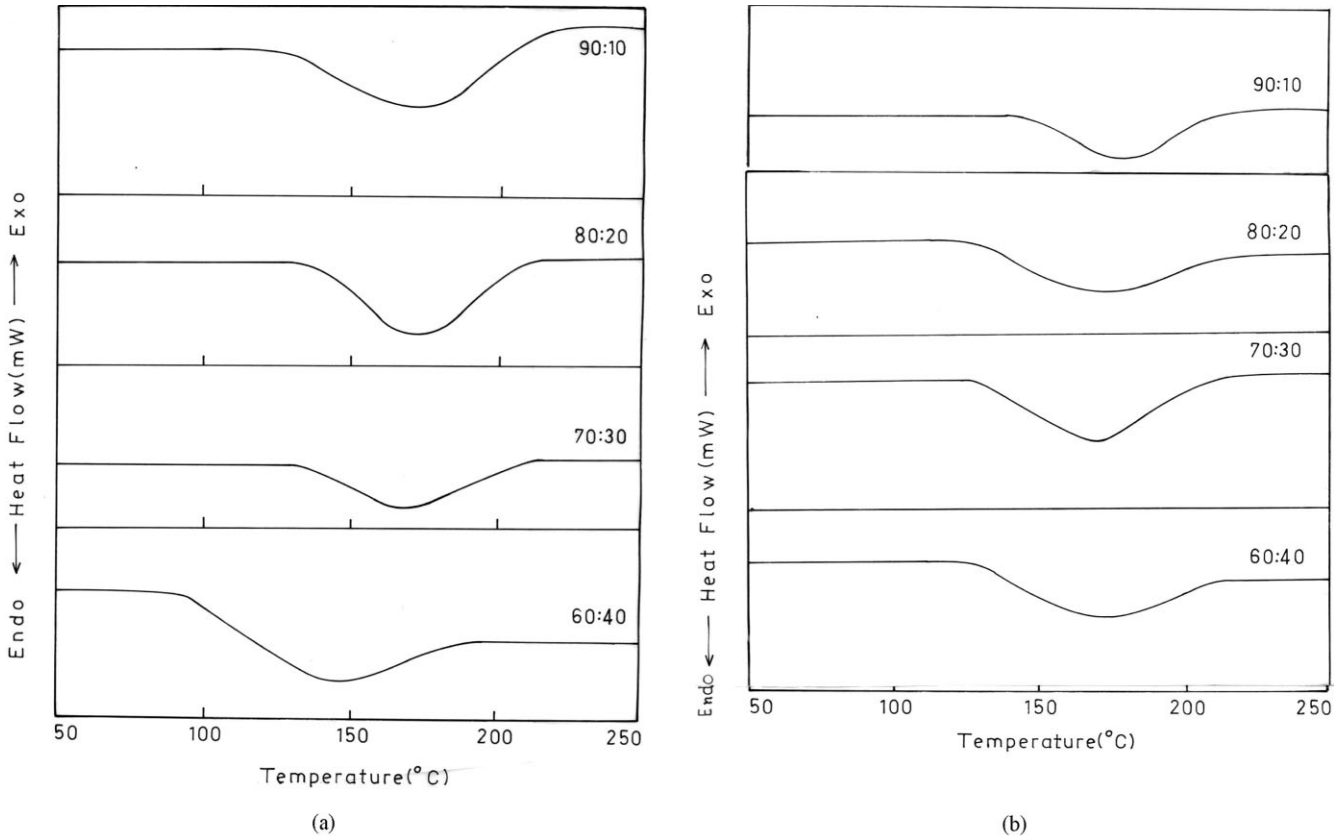

Figure 10 (a) DSC curves for novolac-PBMA semi IPNs. (b) DSC curves for novolac-PBMA full IPNs.

In the present study, the growth of the two polymeric components occurs by two different noninterfering mechanisms, P(*n*-BMA) by a fast free radical polymerization mechanisms and conversion of novolac to phenolic resin by a slower step-growth process. However, the polymerization of acrylic monomer starts at lower temperature (<80°C) when compared with the crosslinking temperature (160°C) of the novolac resin. The increase in gel time for the semi IPNs when compared with pure phenolic may be attributed to shielding effect on the reactive methylol groups imposed by this formerly produced P(*n*-BMA)/*n*-BMA mixture and thus not allowing the -CH_2OH groups of novolac to form the desired methylene and oxymethylene bridges between the novolac chains. This dilution effect of the crosslinking site has further been reflected in the mechanical properties of the resulting IPNs. This effect becomes more and more pronounced as the proportion of *n*-BMA increases. The "autoacceleration effect" as normally encountered with pure homogeneous acrylic polymerization[15] is expected to be reduced remarkably possibly because of the arrest of polymer–monomer mixture within the statistically formed occasional crosslinks of the phenolic network, which restricts the mobility of the monomer molecules. The quicker gelling of the semi IPNs over the full ones may be attributed to the extensive threading or interpenetrating influence of the linear P(*n*-BMA) molecules, which raises the viscosity of the system. The effect (more) presumably offsets the effects of crosslinked P(*n*-BMA) in full IPNs.

FTIR studies

A comparative study of the pattern of depletion of primary alcoholic group (—CH_2OH) characterizing the novolac molecule and that of the same in presence of an *in situ* formed linear P(*n*-BMA) resin has been depicted in the FTIR spectra [Figs. 9(a) and 9(b)] representing pure phenolic crosslinking in a homogeneous phase and that of the same while forming IPN in presence of linear P(*n*-BMA) resin respectively.

The spectra reveals it clearly that within the time scale of experiment, the phenolic crosslinking appears to be complete and uniform in an homogeneous phase while the same in the presence of P(*n*-BMA) appears to be somewhat delayed although the relative amount of —CH_2OH concentration in an IPN is definitely less than that in the pure homogeneous phase.

It is found from the spectra that the peak at wave length of 1373 cm^{-1} almost disappears completely in case of pure phenolic resin, while the same in case of IPN (semi type) is yet to be extinguished. This corroborates our observation on the gelling time as explained

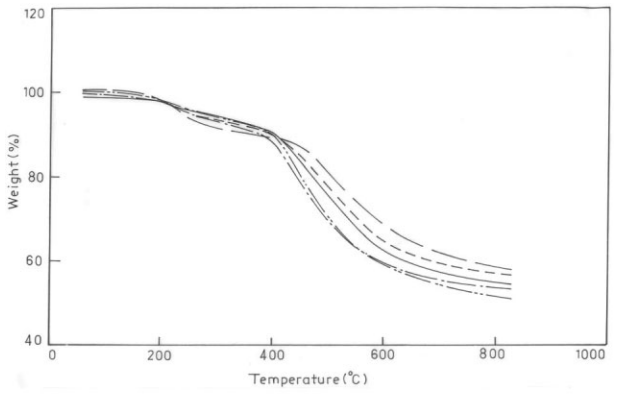

(a)

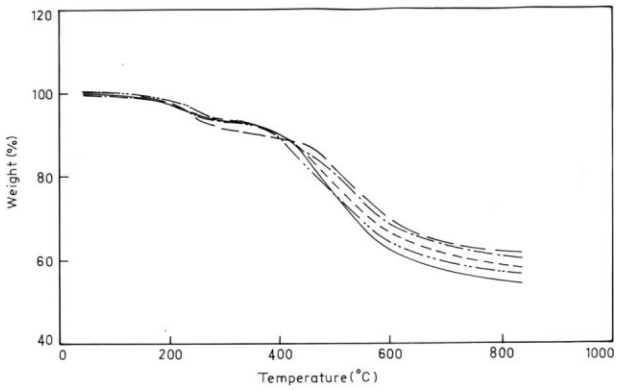

(b)

Figure 11 (a) TGA thermograms of novolac-PBMA semi IPNs: pure PF (— —); PF-PBMA (90:10) (— — —); PF-PBMA (80:20) (——); PF-PBMA (70:30) (— – —); PF-PBMA (60:40) (— – – —). (b) TGA thermograms of novolac-PBMA full IPNs; pure PF (— —); PF-PBMA (90:10) (— – —); PF-PBMA (80:20) (— —); PF-PBMA (70:30) (— – – —); PF-PBMA (60:40) (——).

earlier where we can see a prolonged gel time with the IPN relative to the pure phenolic. The peak at 1456 cm^{-1} has been found to remain almost unaltered in all the cases indicating no change in phenolic —OH group with progress of crosslinking reaction.

Thermal properties

Differential scanning calorimetry

DSC traces of different compositions of semi and full IPNs are exhibited in Figures 10(a) and 10(b) respectively. Because of the restricted mobility of the crosslinked network of P(*n*-BMA) in full IPNs when compared with that of linear chains in semi IPNs, the T_g values of full IPNs are generally higher. The gradual broadening in the endothermic enthalpy change region with increase in P(*n*-BMA) concentration is evident in this study. Also, the extent of phase mixing in case of full IPNs is more than that for semi IPNs. Inclusion of softer elastomeric P(*n*-BMA) domain in brittle phenolic resin has definitely plasticized and toughened the later, as it is observed from the inward shift in T_g values for all the IPNs with respect to that of pure crosslinked phenolic resin (observed T_g, 225°C).

Thermogravimetric analysis

TGA thermograms of both semi and full IPNs are depicted in Figures 11(a) and 11(b) respectively. The onset of degradation of the different IPN systems appears to be slightly accelerated when compared with that of pure phenolic resin (200°C). Although not so pronounced, the individual IPN systems exhibit gradually decreasing onsets with increasing proportion of P(*n*-BMA).

At temperatures around 210°C, both the IPN systems appear to exhibit somewhat increased stability than the pure phenolic resin, irrespective of their compositions and types. In case of both the semi and full IPNs, the stability is found to increase with increase in proportion of P(*n*-BMA) within the range of concentration under study.

Beyond 418°C, both semi and full IPNs are found to degrade at a much faster rate than the pure phenolic resin and clearly exhibit decreased thermal stabilities at elevated temperatures considered in the present case. The pattern of decreasing thermal stability with increasing concentrations of P(*n*-BMA) is almost identical for both semi and full IPNs and here also the higher the proportions of P(*n*-BMA), the lower is the stability. However, there is as such no difference between the thermal stabilities of semi and full IPNs over the entire composition. This trend in thermal stabilities of these IPNs shows that the effect of interpenetration in the case of semi IPNs is nearly counterbalanced by the combined effects of crosslinking and interpenetration as it occurs with the full IPNs.

The depolymerization of P(*n*-BMA) by an unzipping mechanism yields 100% monomer[16] as shown in Scheme 1 later:

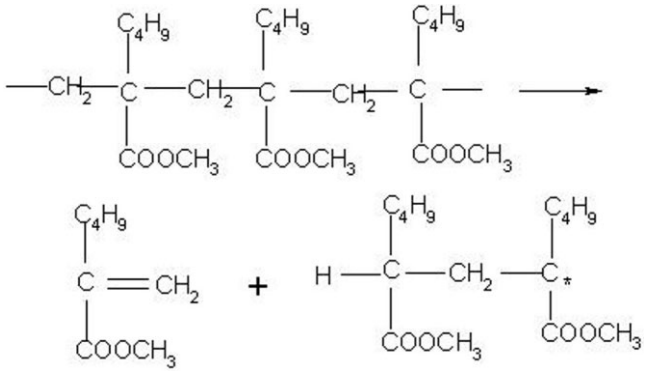

Scheme 1

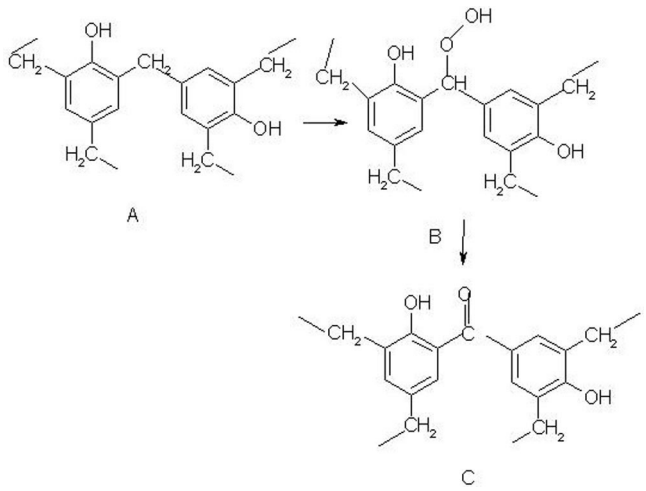

Scheme 2

On the other hand, from low-temperature studies[17–19] the course of degradation of phenolic resin was found to be primarily oxidation at the bridging methylene linkages (Scheme 2) followed by oxidation[20] to form quinone type structure ("G" in Scheme 3).

Thermal degradation of phenolic resin resulting in the formation of quinonoid structure ("G") is a slow process and occurs in a stepwise manner. The initial relatively higher thermal stability (up to 200°C) of the various IPN systems (semi or full) over that of pure phenolic may be ascribed to the scavenging of P(*n*-BMA) degraded macroradicals (although small in quantity at this initial stage of degradation) by the statistically small number of the structure "G" (formed *in situ*) (as shown in Scheme 4).[15,21,22]

At elevated temperature, the rate of depropagation of P(*n*-BMA) becomes high as also the comparatively slower generation of the quinonoid structure (G). The relatively poor thermal stability of the IPN systems than that of the pure phenolic at the higher range of temperatures may be attributed to the depletion of the

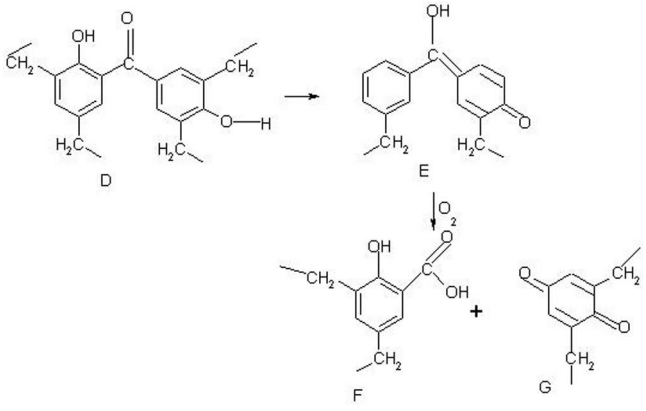

Scheme 3

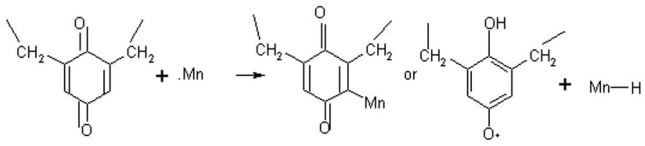

Scheme 4

quinonoid structure at a much faster rate (as shown in Scheme 4) than the rate of generation of P(*n*-BMA) macroradicals, which go on increasing with increasing concentration of P(*n*-BMA) in the IPNs.

Morphology

Scanning electron microscopy

The cocontinuous biphasic micrographs (Fig. 12) of the semi and full IPNs of the system indicate more or less phase separation at an early stage of IPN forma-

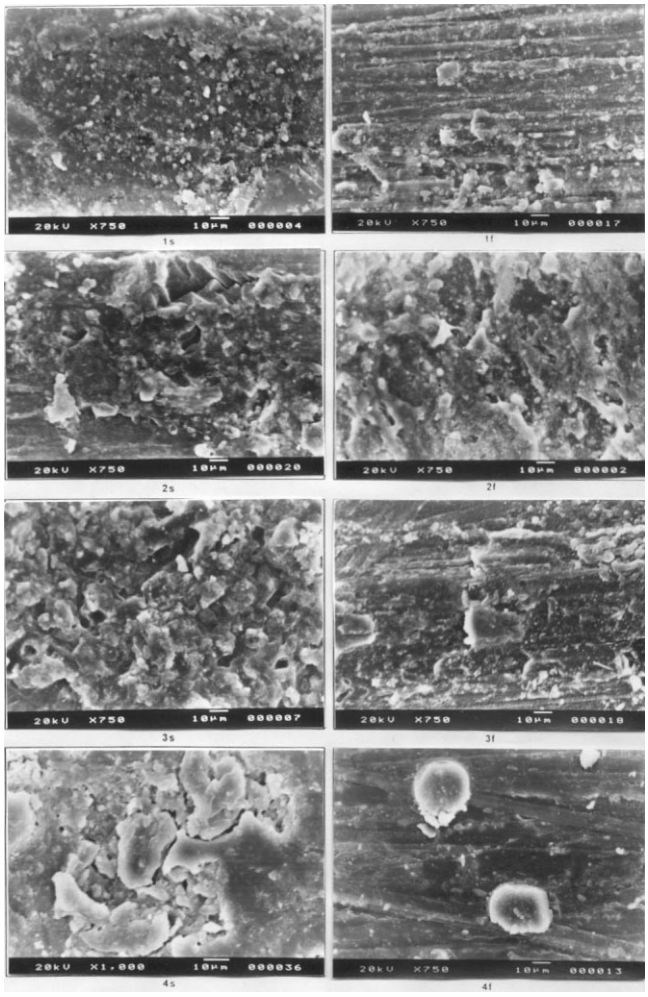

Figure 12 SEM of novolac-PBMA IPNs (×750); sets of micrographs 1s/2s/3s/4s/refer to (90:10)/(80:20)/(70:30)/(60:40) semi IPNs and 1f/2f/3f/4f refer to (90:10)/(80:20)/(70:30)/(60:40) full IPNs respectively.

tion. The small tiny particles of P(*n*-BMA) distributed in a random manner at lower level of P(*n*-BMA) incorporation particularly with semi IPNs are gradually stretched into fibrillar shapes, which exhibit a tendency towards formation of cellular domains as the P(*n*-BMA) content goes on increasing. This leads to the formation of irregularly shaped cellular type structures, which are further deformed by the continuous network of crosslinked phenolic. The overall IPN is also conspicuous by the presence of microvoids all throughout the sample. The typical cellular structure of IPN is found to be initiated relatively at an early stage in the case of full IPN and the cells increase in size with increasing proportion of P(*n*-BMA) but during the later stages i.e., at the highest level of P(*n*-BMA) range of concentration considered in the present study, well defined thick-walled cellular domains are developed. The full IPNs also differ from the semi ones in having compact and dense cellular aggregates.

CONCLUSIONS

A progressive decrease in strength (UTS) and modulus of the IPNs with respect to pure phenolic resin, with increasing P(*n*-BMA) concentration, is evident in this study. Increase in toughness or fracture energy with increase in dispersed P(*n*-BMA) content is always coupled with increase in % E.B. Mechanicals of the full IPNs are superior to those of the corresponding composition of semi IPNs i.e., they possess higher moduli and UTS and consequently lower %E.B. and toughness. These are the direct consequences of the change in crosslink density of the IPNs resulting from the incorporation of P(*n*-BMA) within the novolac matrix. The influence of reduction in crosslink density with increase in P(*n*-BMA) concentration is reflected in the observed trend of changes in hardness also.

A decrease in specific gravity for both semi and full IPNs over those calculated on the basis of simple averages of volume additions for respective compositions is attributed to the imbalance effect of the reduction in specific gravity due to the incorporation of a constituent possessing lower specific gravity, a reduction in compactness of the thermosetting network on one hand, and the increase in specific gravity due to interpenetration or interwinding.

The degree of thermal decomposition of various IPNs were influenced appreciably by the degree of crosslinking of the minor phase as the semi IPNs of all the novolac-P(*n*-BMA) systems were more stable than the full ones.

In all the cases, the course of degradation has involved two distinguishable stages. First, the stepwise unzipping process producing the methacrylate monomer followed by the scavenging of the intermediate methacrylate free radicals by the intermediate compounds (Quinonoid structure of phenolic degradation.

The influence of crosslinking on glass transition temperature is clearly observed from the DSC curves as the full IPNs show higher T_gs than the corresponding semi IPNs along with better phase mixing. This is attributed to the presence of comonomer crosslinker of the P(*n*-BMA) that, besides forming intermolecular crosslinks among the P(*n*-BMA) chains, form homopolymers that lead to better phase mixing.

References

1. Xiao, H. X.; Frisch, K. C.; Koedomenos, C. Z.; Ryntz, P. I. ACS Symp Ser 1988, 367, 1153.
2. Cox, J. A.; Gajck, R. G.; Litwinski, R.; Carnaham, J.; Trochimczuk, W. Anal Chem 1982, 54, 1153.
3. Pozniak, G.; Trochimczuk, W. Angew Makromol Chem 1980, 92, 155.
4. Shalaby, S. W.; Hoffman, A. S.; Ratner, B. D.; Horbett, T. A., Eds. Polymers as Biomaterials; Plenum Press: New York, 1984.
5. Lipatov, Y. S.; Semenovitch, G. M.; Skiba, S. I.; Karabanova, L. V.; Sergeeva, L. M. Polymer 1992, 33, 361.
6. Lin, M. S.; Jeng, K. T. J Polym Sci Part A: Polym Chem 1992, 30, 1941.
7. Lin, M. S.; Lee, S. T. Polymer 1995, 36, 4567.
8. Bauer, B. J.; Jackson, C. L.; Liu, D. W. In Proceedings of MRS Meeting, San Francisco, CA, April 1995.
9. Bauer, B. J.; Jackson, C. L.; Liu, D. W. In Proceedings of ACS-APS Intersociety Meeting, Baltimore, MD, October 1995.
10. Bauer, B.; Briber, B. R.; Dickens, B. Adv Chem Ser 1995, 239, 179.
11. Klempner, D.; Frisch, K. C. J Elastoplast 1973, 5, 196.
12. Fradkin, D. G.; Foster, J. N.; Sperling, L. H. Rubber Chem Technol 1986, 59, 255.
13. Foster, J. N.; Sperling, L. H.; Thomas, D. A. J Appl Polym Sci 1987, 33, 2637.
14. Homan, J. G.; Yu, X. H.; Connor, T. J.; Cooper, S. L. J Appl Polym Sci 1991, 43, 2249.
15. Odian, G. In Principles of Polymerisation, 2nd ed.; Wiley: New York, 1981; p 244.
16. Mcneil, I. C. In Developments in Polymer Degradation-1; Grassie, N., Ed.; Applied Science: Essex, UK, 1977; Chapter 6.
17. Frisch, K. C.; Klempner, D.; Frisch, H. L.; Ghiardella, H. In Recent Advances in Polymer Blends, Grafts and Blocks; Sperling, L. H., Ed.; Plenum: New York, 1974.
18. Conley, R. T.; Bieron, J. F. J Appl Polym Sci 1963, 7, 103.
19. Conley, R. T.; Bieron, J. F. J Appl Polym Sci 1967, 7, 171.
20. Grassie, N.; Scott, G. Polymer Degradation and Stabilisation; Cambridge University Press: Cambridge, UK, 1985; p 24.
21. Goswami, S.; Chakraborty, D. J Appl Polym Sci 2004, 94, 2764.
22. Goswami, S.; Bandyopadhyay, D.; Mandal, P. K.; Chakrabarty, D. J Appl Polym Sci 2003, 90, 412.
23. Morrell, S. H. In Rubber Technology and Manufacture, 2nd ed.; Blow, C. M., Hepburn, Eds.; Butterworth Scientific: UK, 1982; p 189.